JOURNAL OF CATALYSIS 77, 473–484 (1982)

The Properties of Heteropoly Acids and the Conversion of Methanol to Hydrocarbons

H. HAYASHI[1] AND J. B. MOFFAT[2]

Department of Chemistry and Guelph–Waterloo Centre for Graduate Work in Chemistry, University of Waterloo, Waterloo, Ontario N2L 3G1, Canada

Received February 24, 1982; revised April 6, 1982

The properties of the heteropoly acids, 12-molybdophosphoric acid, 12-tungstosilicic acid, and 12-tungstophosphoric acid, and the dimeric 9-tungstophosphoric acid have been examined. The conversion of methanol to hydrocarbons has been employed as a test reaction for the activity and selectivity of these catalysts. The effects of variations in reaction temperature, calcination temperature, and environment (air, helium, hydrogen), and residence time have been studied, and the catalysts have been characterized by measurements of surface area, pore size distributions, X-ray powder diffraction, and the chemisorption of ammonia.

INTRODUCTION

Interest in this laboratory has centered on stoichiometric and nonstoichiometric acidic heterogeneous catalysts, particularly those containing phosphorus, oxygen, and one other element, the latter usually a metal (*1*). Initially our attention was focused on those catalysts where the third element is boron, but more recently work has been extended to include a variety of metals as the third element (*2*). It appeared both interesting and worthwhile to expand the study to include those solid acidic catalysts where four elements are present. Among such catalysts are the so-called heteropoly acids.

The synthesis of various heteropoly acids dates back to as early as 1826 (*3*), but studies of their properties are of more recent vintage. Tsigdinos has recently published several excellent comprehensive reviews of heteropoly compounds (*4, 5*). Although some reports of the catalytic properties of the heteropoly compounds, particularly those containing molybdenum, appeared over 10 years ago (*6, 7*), it is only in the last several years that the interest in this aspect has intensified. The 12-molybdophosphoric acid and its salts have been shown to be active in the oxidation of methacrolein (*8*) and infrared spectroscopy has been employed to show that this heteropoly acid owes its acidic properties almost entirely to Brønsted sites (*9*). Heteropoly acids and their salts are also effective catalysts for liquid-phase reactions such as the oxidation of olefins (*10*), the hydration of olefins (*11*), the polymerization of benzyl alcohols (*12*), and the alcoholysis of epoxide (*13*). Temperature-programmed reduction combined with infrared spectroscopy has been used to study the effect of hydrogen treatment on 12-molybdo- and 12-tungstophosphoric acids (*14*). Heteropoly acids (*15*) and the copper and silver salts of 12-tungstophosphoric acid (*16*) have very recently been shown to have activity for the conversion of methanol to hydrocarbons.

The present work involves the 12-molybdophosphoric, 12-tungstosilicic, and 12-tungstophosphoric acids and the dimeric 9-tungstophosphoric acid. The study employs the methanol conversion to hydrocarbons as the test reaction for measuring the activity and selectivity of these catalysts. The

---

[1] On leave from Department of Chemical Engineering, Tokushima University, Minamijosanjima, Tokushima 770, Japan.

[2] To whom correspondence should be addressed.

0021-9517/82/100473-12$02.00/0

effects of variations in reaction temperature, calcination temperature and conditions (air, helium, hydrogen), and residence time have been studied, and the catalysts have been characterized by measurements of surface area, pore size distributions, X-ray powder diffraction, and the chemisorption of ammonia.

EXPERIMENTAL

Apparatus and procedure. Methanol conversion was carried out in a microcatalytic pulse reactor. Catalyst powder was packed in a short section of $\frac{1}{4}''$ stainless-steel tubing. At the inlet of the reactor, carrier gas (helium, 30 ml/min) was split into two streams, one of which was passed through the catalyst bed and the remainder by-passed the reactor. The flow rate of the reactor-helium was adjusted to a given value using a calibrated glass-capillary/dibutyl phthalate manometer and a needle valve. The by-pass stream and that exiting from the reactor were joined together and lead to the column for analysis of the products by gas chromatography. Apparent residence time (W/F) is defined in this paper to be the ratio of catalyst weight (W) and flow rate of reactor helium (F). Prior to the start of the reaction, the catalyst was heated up to the reaction temperature in a flow of helium, which was vented before the inlet of the column. During the preconditioning period the gas chromatograph was operated separately. After switching to the analysis mode, an aliquot of methanol (2 μl = 49.4 μmol) was injected through a septum at the top of the reactor and the products were analyzed directly. Attempts were made to analyze after trapping by liquid-nitrogen but it was found that methane and carbon monoxide passed through the trap. Methanol, dimethyl ether, carbon monoxide, carbon dioxide, and C_1–C_3 hydrocarbons were analyzed by $\frac{1}{4}''$ × 10 ft Porapak Q at 70°C and C_4–C_6 hydrocarbons by a series column of $\frac{1}{8}''$ × 1.7 ft Durapak (Carbowax 400/Porasil C) and $\frac{1}{4}''$ × 10 ft 15% Squalane/Chromosorb W at 50°C. Yields are expressed on a carbon-number basis.

Materials. 12-Tungstophosphoric and 12-molybdophosphoric acids were obtained from BDH Chemicals. 12-Tungstosilicic acid was Baker analyzed reagent. Dimeric 9-tungstophosphoric acid was prepared in our laboratory after Wu (*17*). The method employed for the determination of tungsten and phosphorus in these heteropoly acids will be published elsewhere (*18*). Methanol was Baker Photrex grade reagent. Dimethyl ether and other gases were obtained from Matheson as CP grade in lecture bottles. All chemicals and gases were used as received.

Characterization of catalysts. Pore size distribution and surface area were measured with a Micromeritics Autopore 9200, where the contact angle and surface tension of mercury were taken to be 140° and 485 dyn/cm, respectively. Acid strength was determined by the indicator method (*19*). Indicators (p*K*a) used were: Benzeneazodiphenylamine (+1.5), Dicinnamalacetone (−3.0), Benzalacetophenone (−5.6), and Anthraquinone (−8.2). Total amounts of acidic site were estimated from the chemisorption of ammonia at room temperature using a quartz-spring balance. An aliquot of sample was evacuated overnight and after equilibrating at 350 ~ 400 mm Hg of ammonia pressure was again evacuated overnight to a constant weight. Powder X-ray diffraction employed a Phillips diffractometer (Model PW-1011/60) at 40 kV and 30 mA with Cu*K*α radiation.

RESULTS

Thermal Stability of Heteropoly Acids

Heteropoly acids are known to be highly hydrated. Various amounts of water of crystallization, n = 30 (*20*), 29 (*5, 21*), 27.5 (*22*), and 24 (*20*) for $H_3PW_{12}O_{40} \cdot nH_2O$ at room temperature, have been reported. Freshly recrystallized 12-tungstophosphoric acid is expected to be 29-hydrate, which was confirmed by X-ray structural

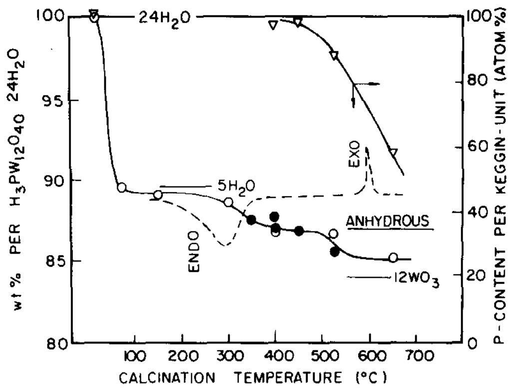

FIG. 1. Decrease in weight and phosphorus content in calcination of $H_3PW_{12}O_{40} \cdot 24H_2O$. ○, Calcined in air for 3 hr (static); ●, calcined in helium for 2 hr (flow); X, phosphorus content; dashed line, DTA by West and Audrieth (*25*).

analysis (*21*), and readily converts to 24-hydrate on standing (*20*). As pointed out by Tsigdinos (*5*), some of the differences in the reported thermograms and hydration numbers may be due to failure to attain equilibrium conditions (*22, 23*).

Figure 1 shows the weight loss in calcination of $H_3PW_{12}O_{40} \cdot 24H_2O$, where an aliquot of the hydrate was heated in air for 3 hr (static) and in helium for 2 hr (flow) at a given temperature. Phosphorus content of the starting hydrate by EDTA-analysis (*18*) was 1.01_5 atom/Keggin unit as 24-hydrate. Weight loss was observed in three stages. The first stage shows the removal of zeolitic water to give the 4 ~ 5-hydrate. Keggin (*24*) obtained 5-hydrate over phosphorus pentoxide. The second stage shows the formation of anhydrous acid at 350 ~ 450°C in good agreement with the differential thermal analysis (DTA) reported by West and Audrieth (*25*). Powder X-ray data given in Fig. 2 shows broadening and decrease in intensity at temperatures around 400°C, but provides evidence for retention of the heteropoly structure. Further weight loss and substantial change in the X-ray pattern were observed at temperatures above 525°C. Although DTA data (*25*) suggest the heteropoly structure of 12-tungstophosphoric acid decomposes at 600°C, our results show the decomposition starts as low as 500°C in the case of prolonged heating. The weight loss in this high-temperature region was attributed to loss of phosphorus as evident from the results shown in Fig. 1. The phosphorus is presumably lost through the sublimation of P_2O_5.

Pore Size Distribution and Surface Area

X-Ray structural analysis (*21*) for $H_3PW_{12}O_{40} \cdot 29H_2O$ shows $[PW_{12}O_{40}]^{3-}$ and $[H_3 \cdot 29H_2O]^{3+}$ occur alternately at the corners of the body-centered cubic lattice. Both the heteropoly anion and $29H_2O$ are close to 10 Å in diameter if assumed to be spherical. Water molecules in the interstices between heteropoly anions show zeolitic behavior and can be removed on heating without change in crystal structure. Thus it has been believed that calcined heteropoly acids should be very porous with high-surface area (*25*).

However, the surface area of calcined 12-tungstophosphoric acid as measured by mercury porosimetry was relatively low, ranging around 4 ~ 5 m^2/g as shown in Table 1. If the water molecules were removed without change in the arrangement of heteropoly anions the surface area can be estimated to be as high as 650 m^2/g based on the formula weight and diameter of $[PW_{12}O_{40}]^{3-}$, 2877 and 10 Å, respectively. Since the pore radii reported here are confined to a range with a minimum value of 15 Å, the surface area as measured by mercury penetration may be somewhat low. The N_2BET area was, however, found to be approximately the same as that found by porosimetry (Table 1). In contrast with expectation (*25*), the surface area of calcined 12-tungstophosphoric acid (4 ~ 5 m^2/g) was lower than that of uncalcined 24-hydrate (7.9 m^2/g), suggesting that pore shrinkage or collapse has occurred during the removal of water molecules.

Figure 3 shows pore size distribution for 12-tungstophosphoric acid. The distribution curves were apparently trimodal: Nar-

TABLE 1

Properties of Heteropoly Acids

Heteropoly acid	Calcination temperature (°C)		Hydration level	Color	Surface area (m²/g)[a]	Chemisorbed NH_3(meq/g)[b]	Acid strength H_0[c]			
							+1.5	−3.0	−5.6	−8.2
$H_3PW_{12}O_{40}$	—		$24H_2O$	White	7.8$_5$		+	+	−	−
	70	air		White			+	+	+	−
	150		Fig. 1	White	4.7$_4$		+	+	+	−
	300			White (δ-gray)		0.82				
	400			White (δ-gray)		0.58				
	525			Olive green						
	650			Dark green	3.8$_6$					
	300	He		White (δ-gray)			+	+	+	+
	350			White (δ-gray)		1.48				
	400			White (δ-gray)	4.5$_2$ (3.1)[d]	1.18 ~ 1.50	+	+	+	+
	450			White (δ-gray)		1.62	+	+	+	(−)
	525			White (δ-green)			+	+	(−)	×
	350	H_2		Deep gray		1.22				
	400			Black						
	450			Black		1.19				
$H_3PMo_{12}O_{40}$	—		$24H_2O$	Yellow			+	(−)	×	×
	350	He	anhydrous	Yellow (δ-green)	6.7$_7$		+	+	×	×
	350	H_2		Black						
$H_4SiW_{12}O_{40}$	—		$22.5H_2O$	White			+	+	−	−
	400	He	anhydrous	White (δ-gray)	5.5$_1$	1.99	+	+	+	−
$H_6P_2W_{18}O_{62}$	—		$35H_2O$	White (δ-yellow)			+	+	×	×
	400	He	anhydrous	Yellow (δ-green)	4.6$_0$		+	+	×	×
	400	H_2		Black	8.8$_2$					

[a] Porosimetry.

[b] Adsorption at room temperature, evacuated overnight.

[c] Measured by indicator method. +, Acidic color; −, basic color; ( ), vague; ×, not measurable.

[d] BET area.

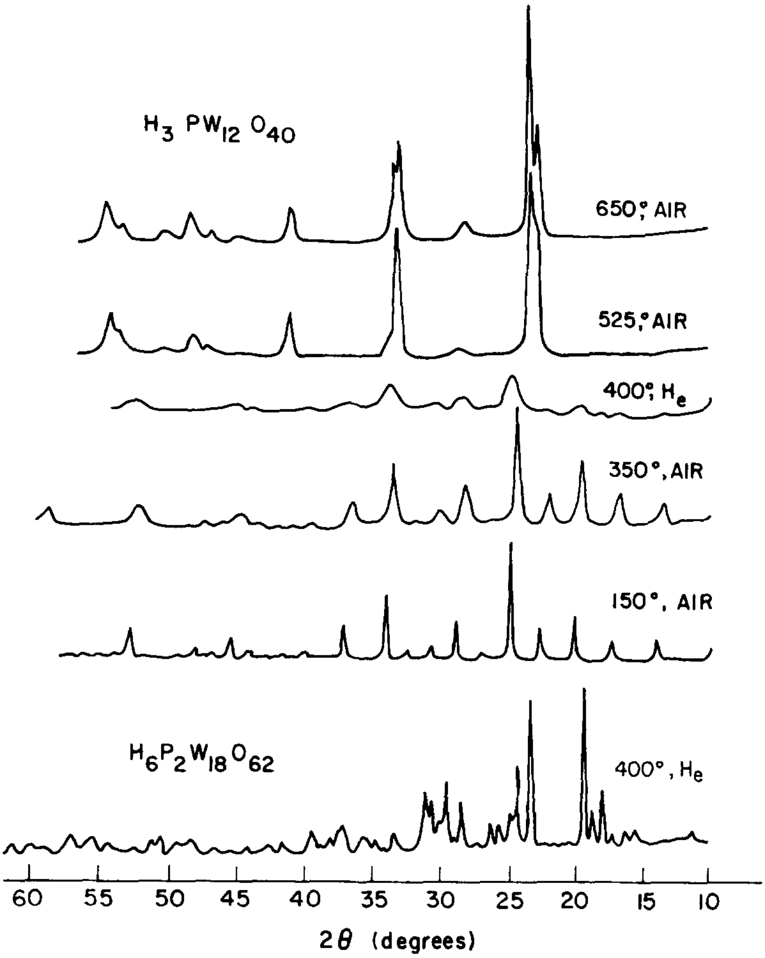

FIG. 2. Powder X-ray patterns for $H_6P_2W_{18}O_{62}$ and $H_3PW_{12}O_{40}$ calcined at various conditions.

rower pores below the limit of porosimetry (<15 Å), intermediates 30 Å range, and large pores at 70–100 Å in radius. Both the peak at approximately 30 Å and that in the vicinity of 80 Å shifted to lower radii on heating. The peak at 30 Å suffered a significant decrease in magnitude, while that at 80 Å remained essentially the same. Such results presumably result from a shrinkage in pores but also the collapse (to values at least less than 15 Å in radii) of the smaller sized pores. It is important to note, however, that at very high pressures, structure collapse and mercury compression may introduce errors into the results obtained by mercury porosimetry.

Acidic Properties

The acid strength of heteropoly acids measured by the indicator method and the amounts of ammonia chemisorbed are summarized in Table 1. Anhydrous $H_3PW_{12}O_{40}$ was shown to be strongly acidic with H_0 values as low as −8.2. The acid strength decreased on hydration: the maximum p*K*a was −5.6 and −3.0 for 5-hydrate and uncalcined 24-hydrate, respectively. Amounts of ammonia chemisorbed at room temperature on $H_3PW_{12}O_{40}$ calcined at 350 ~ 450°C in helium were 1.2 ~ 1.6 meq/g, somewhat higher than the 1.0_4 meq/g expected as tribasic acid. Similar results were obtained for

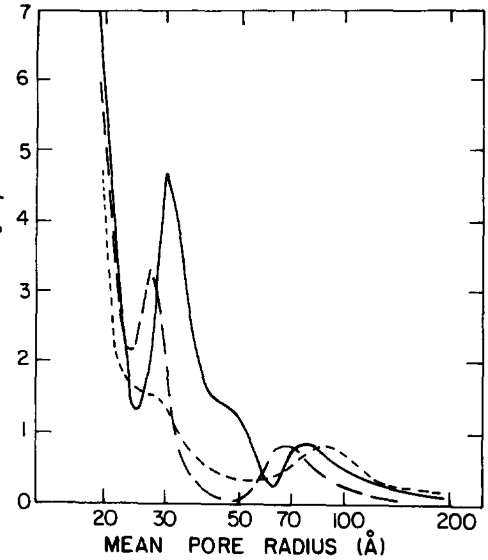

FIG. 3. Pore size distribution of $H_3PW_{12}O_{40}$. ——, Uncalcined, $24H_2O$; – – –, calcined at 150°C in air, $5H_2O$; ··· calcined at 400°C in helium, anhydrous.

$H_4SiW_{12}O_{40}$, but it was impossible to determine the maximum acid strength of the colored acids of $H_3PMo_{12}O_{40}$ and $H_6P_2W_{18}O_{62}$.

Equilibrium Conversion of Methanol to Dimethyl Ether

As will be discussed in the subsequent section, methanol conversion into hydrocarbons appears to pass through dimethyl ether (DME) as an intermediate. The equilibrium constants for the reaction

$$2CH_3OH \rightleftarrows CH_3OCH_3 + H_2O \qquad (1)$$

may be expressed as

$$Kp = \frac{1}{4}\left(\frac{X_{Ae}}{1 - X_{Ae}}\right)^2 \qquad (2)$$

where X_{Ae} represents the equilibrium fractional conversion of methanol, and water is assumed to be produced stoichiometrically with DME. Since thermodynamic properties at 25°C (*26*) and heat capacity data at higher temperatures (*27–29*) are available for the species involved in process (1), an equation relating the equilibrium constant to the temperature can be obtained as

$$-R \ln Kp = \frac{\Delta G}{T} = \frac{-6836}{T} + 3.32 \ln T - 0.475 \times 10^{-3}\, T - 0.11 \times 10^{-6}\, T^2 - 10.92. \qquad (3)$$

Strongly acidic, free heteropoly acids were too active for measuring the equilibrium behavior due to further conversion into hydrocarbons, and $Na_3PW_{12}O_{40}$ was used for this purpose. The results are given in Fig. 4, covering a wide range of residence times. The dashed line in the figure shows the equilibrium conversion of methanol to dimethyl ether as estimated from Eqs. (2) and (3). For the initial pulse of methanol, conversion of methanol (X_A) was a little higher than the expected yield of dimethyl ether (Y_E) presumably due to irreversible adsorption on fresh catalyst. For the second and third pulse, with increasing residence time, fairly good agreement of X_A and Y_E was observed, showing the dehydration reaction (1) occurred exclusively. For small residence times no hydrocarbons are formed on $Na_3PW_{12}O_{40}$, but as the residence time increases beyond 100 (mg-cat min/ml-He), the quantity of hydrocarbons produced increases. It appears that the discrepancy between the values obtained for X_A and Y_E at pulse number 4 may, at least in

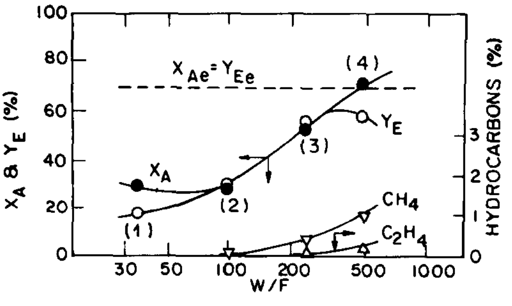

FIG. 4. The approach to equilibrium between methanol and dimethyl ether in the conversion of methanol. Catalyst, $Na_3PW_{12}O_{40}$ calcined at 400°C in helium; temperature, 352°C; pulse size, 2 μl methanol; numerals in parentheses show the sequence of pulse numbers; ●, X_A, conversion of methanol; ○, Y_E, yield of dimethyl ether.

part, be due to such hydrocarbon formation.

Formation of Hydrocarbons

Dimethyl ether was obtained in high yield approaching the equilibrium value and the yield passed through a maximum as shown in Fig. 4 for the sodium salt. The residence time at which hydrocarbons just appeared was close to that of the maximum yield of dimethyl ether. The yield pattern from dimethyl ether was quite similar to that from methanol as compared in Fig. 5 for $H_3PW_{12}O_{40}$, suggesting hydrocarbons were formed through dimethyl ether.

Figure 6 shows the effect of residence time on the yield pattern at different temperatures, providing a qualitive picture for the reaction path in methanol conversion. A similar pattern has been given by Chang and Silvestri (*30*) for the same reaction over ZSM-5 zeolite. Hydrocarbon formation was observed at a lower residence time region for the strongly acidic $H_3PW_{12}O_{40}$ than observed with the sodium salt. At the lowest temperature (325°C) there is evidence for the formation of hydrocarbons at a residence time of 100 mg-cat min/ml-He. A maximum appears for CH_4, C_2H_4, and C_3H_8 in the range between 100 and 1000 for W/F. The quantity of methane formed is greater than that of any of the other hydrocarbons, although at the highest residence times propane is produced in approximately equal amounts. The quantity of ether decreases continuously and sharply as W/F increases while the conversion of methanol exceeds 90% with all three reaction temperatures. At 352°C reaction temperature ethylene appears as the dominant hydrocarbon although methane is produced in almost

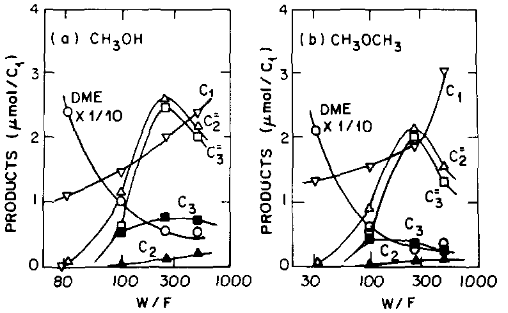

FIG. 5. Product yields from methanol (a) and dimethyl ether (b) at various residence times. Catalyst $H_3PW_{12}O_{40}$ calcined at 350°C in helium; reaction temperature, 352°C; pulse size, 49.4 µmol/C_1; W/F, apparent residence time in mg-cat min/ml-He.

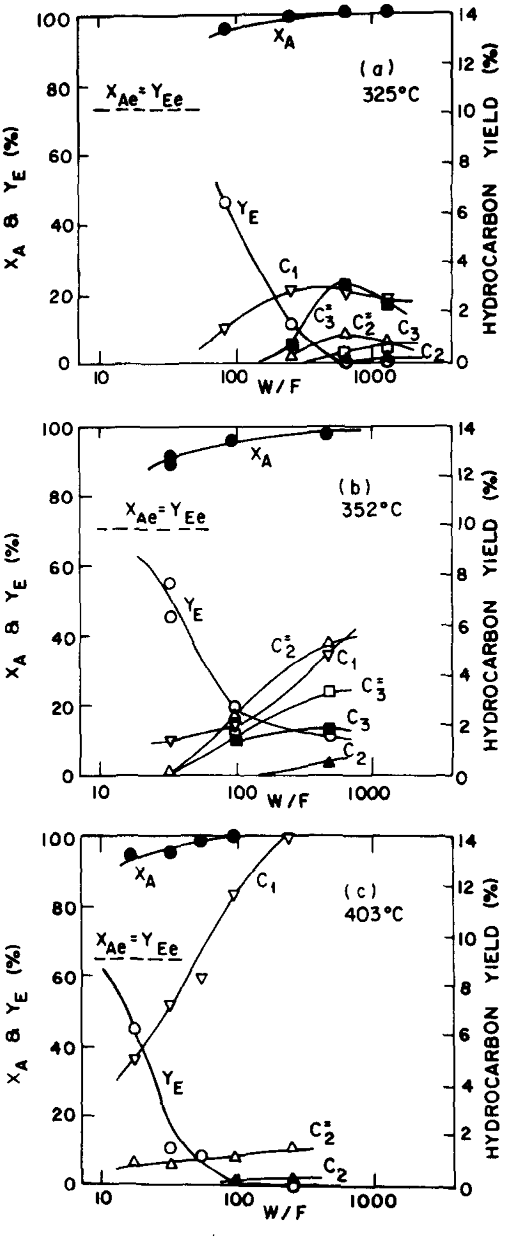

FIG. 6. Effect of residence time on the conversion of methanol over $H_3PW_{12}O_{40}$ at various temperatures. W/F, apparent residence time in mg-cat min/ml-He; dashed lines, equilibrium for DME formation.

equal amounts. At this reaction temperature hydrocarbons begin to appear at a W/F of 20. A maximum in the hydrocarbon concentrations has not appeared up to a W/F value of 500. The quantities of each hydrocarbon produced at 352°C are in general higher than those found at 325°C. At 403°C the quantities of methane produced are considerably higher than those at the two lower temperatures, no significant amounts of C_3 hydrocarbons form and no maxima in the hydrocarbon yields appear up to W/F equal to 500.

Thermogram and powder X-ray data given in Figs. 1 and 2 suggest that $H_3PW_{12}O_{40} \cdot 24H_2O$ forms anhydrous free acid at 350–450°C without decomposition of the heteropoly structure. However, hydrocarbon yields were strongly affected by the calcination temperature and environment as shown in Fig. 7, where the reaction was carried out at the same temperature of 352°C. Under all calcination environments and temperatures, the conversion of methanol at 352°C is greater than 90%, while the quantities of DME produced at low residence times (W/F equal to approximately 30) range from 30 to 60%. With those catalysts calcined in helium the yields of hydrocarbons vary considerably with temperature. The maximum in the yields of hydrocarbons obtained after 350°C calcination in helium evidently shifts to higher W/F values as the calcination temperature is increased. With both the 350 and 400°C calcination temperatures in helium the C_4 hydrocarbons appeared in larger amounts than any of the other measured hydrocarbons, while with the 450°C calcination temperature (in helium), methane is produced in the largest quantities. In contrast, the use of the 450°C calcination temperature with a hydrogen environment again elevated the C_4 hydrocarbon to the highest concentration, with a maximum appearing at a W/F of approximately 100. The maxima observed in the yields of hydrocarbons after calcination at 350°C in helium are also observed

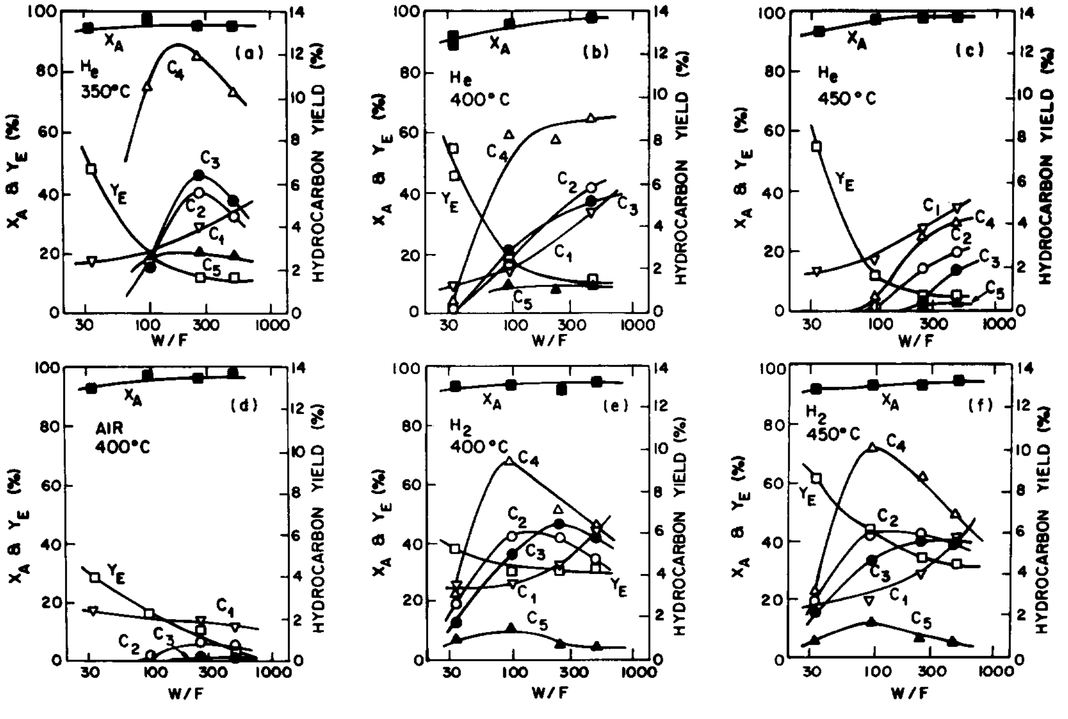

FIG. 7. Effect of calcination conditions on the conversion of methanol over $H_3PW_{12}O_{40}$ at 352°C. W/F, apparent residence time in mg-cat min/ml-He.

with those catalyst calcined at 400 and 450° C in hydrogen. The air-calcined catalyst produced the smallest yield of dimethyl ether as well as hydrocarbons, and methane again appeared as the hydrocarbon of highest concentration.

Similar effect of calcination condition was observed for dimeric 9-tungstophosphoric acid. $H_6P_2W_{18}O_{62}$ calcined at 400°C in helium showed 99% conversion of methanol at 352°C and W/F = 100 mg-cat min/ml-He, and gave 56% yield of dimethyl ether with 5.5% CO and 0.9% CO_2, where no hydrocarbons were detected except 1.2% CH_4. Hydrogen-calcined dimeric acid produced 4.1% CH_4, 6.1% C_2H_4, 9.1% C_3H_6, 13.7% C_4, and 8.7% C_5 without great change in the methanol conversion (94%) and the yield of dimethyl ether (42%) at the same reaction condition.

12-Molybdophosphoric acid gave carbon monoxide as high as 62% in yield at 350°C, presumably due to the oxidation of methanol through formaldehyde, and no hydrocarbons were detected. The behavior of $H_4SiW_{12}O_{40}$ was similar to that of $H_3PW_{12}O_{40}$.

Product Behavior

The results given in Figs. 5–7 for methanol conversion over $H_3PW_{12}O_{40}$ may be summarized as follows in terms of the product behavior. (i) Methane increased with the increase in residence time, while olefins passed through a maximum and paraffins showed a plateau. The formation of methane appears to be different in mechanism from that of other hydrocarbons. Subsequent reactions of the olefins may lead to a decrease in their yield at higher residence time regions. (ii) The residence time at which hydrocarbons show maxima in their yield was affected by the calcination conditions, but seems to move together regardless of the carbon number, suggesting the decomposition of dimethyl ether to be rate-determining. (iii) Methane is the predominant product at a higher temperature of 403° C. Formation of C_3–C_5 hydrocarbons was observed at 352°C, where the product distribution showed a maximum of C_4 and suddenly decreased above C_5, in good agreement with the literature data (*15*). (iv) High values for hydrocarbons in methanol conversion over heteropoly acids are given in the literature (*15, 16*). However, it should be noticed that they are not absolute yields but product distributions among *detected* hydrocarbons. Mass balances demonstrate the irreversible adsorption and/or decomposition of presumably higher hydrocarbons on the surface of the catalyst, the latter evidenced by the black color of the catalysts recovered after reaction. (v) High conversion of dimethyl ether does not always result in an increase in the yield of detectable hydrocarbons. Figures 7c and d show higher conversion of ether with lower yield of hydrocarbons, and vice versa in Figs. 7e and f.

As the catalyst is strongly acidic, it seemed likely that cracking of longer chain hydrocarbons rapidly formed on the surface was involved as a possible route to afford C_3–C_5 hydrocarbons as well as carbon-chain propagation starting from C_1- and/or C_2-species. Thus attempts were made to examine the reactions of some hydrocarbons over $H_3PW_{12}O_{40}$ at 350°C and W/F = 247 mg-cat min/ml-He. Pulse size was adjusted to that of methanol (49.4 μmol). For example, the reaction of isobutylene produced 1.8% CH_4, 0.2% C_2H_4 + C_2H_6, 2.9% C_3H_6 + C_3H_8, 5.8% i-C_4H_{10}, 43.2% i-C_4H_8 + 1-C_4H_8, 16.6% 2-C_4H_8, and 2.3% C_5 with 70.8% recovery. Products were distributed on both sides of carbon number C_4 and the formation of isobutane suggests hydrogenation occurred along with the carbonization. 1-Butene isomerized to 2-butene, and gave C_1–C_5 products similar to isobutylene. Further, propylene gave C_4 and C_5 hydrocarbons, though small in amount. It is impossible to explain the formation of these products without accounting for the rapid propagation of carbon-chain with succeeding cracking reactions. Reactivity of ethylene was rather low. Ethane and propane were recovered without reaction.

Figure 8 shows surface area of fresh $H_3PW_{12}O_{40}$ calcined at 400°C in helium and the recovered catalysts after 30 ≈ 120 pulses of methanol at 350°C. Carbon deposit seems to spread over the surface as fine aggregates.

DISCUSSION

It is quite evidently not yet possible with the information presently available to provide an unambiguous mechanism for the conversion of methanol on heteropoly acids. It is appropriate, however, to provide some conclusions, albeit of a speculative nature, concerning the conversion of methanol on the heteropoly acids studied here. Since the catalysts examined here are strongly acidic, it is highly probable that the active sites in the conversion of methanol are themselves acidic and most likely that carbonium ions play an important role in the process. Since there is no evidence that water, a reaction product from the conversion of methanol, decreases the activity of the catalyst, it must be presumed that the active sites are of Brønsted acidic character.

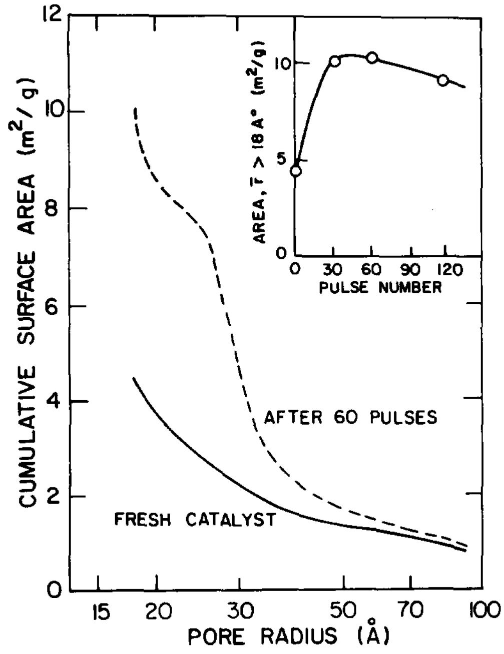

FIG. 8. Variation of surface area by carbonization. Catalyst, $H_3PW_{12}O_{40}$ calcined at 400°C in helium; reaction conditions, 350°C, W/F = 500 mg-cat min/ml-He, 2μl methanol, 1 min-interval; area was measured by mercury porosimetry.

The observation that aliphatic hydrocarbons are recovered unreacted while olefinic hydrocarbons are converted over the heteropoly acids is also suggestive of the active participation of carbonium ions. Since hydrocarbons begin to form as dimethyl ether decreases in concentration, while the amount of methanol remains essentially constant and the product distributions from methanol and dimethyl ether are similar, the conversion of methanol to hydrocarbons appears to take place through dimethyl ether. Since equilibrium quantities of DME can be obtained over the sodium salt, it is concluded that less acidic sites may be sufficient to catalyze the formation of the ether.

It is of interest to note that the maximum observed in the yields of hydrocarbons is found, under a given set of calcination and reaction conditions, with one exception for all measured hydrocarbons, although the residence times at which the maxima appear may not be identical for all hydrocarbons. The exceptional hydrocarbon, methane, has a concentration which increases with residence time on the more active catalysts and continues to increase after the concentration of DME ceases to change with residence time. While CH_4 can be formed directly from the alcohol and/or ether, it evidently may also result from the degradation of the longer chain hydrocarbons, as well as by direct desorption from the surface. Such a behavior is symptomatic of a mechanism involving carbonium ions. For a fixed calcination condition, the amounts of the longer chain hydrocarbons (C_2–C_4) which are produced increase in passing from a 325°C reaction temperature to 352°C, and then decrease markedly at the highest temperature of 403°C. The rate of consumption of DME accelerates with increase in reaction temperature. At the highest reaction temperature the product consists of only C_1 and C_2 with the former predominating. It is apparent that a portion of the product remains irreversibly chemisorbed and/or degraded to carbon on the surface of the catalyst.

Changes in the calcination conditions may alter both the numbers and strengths of the acidic sites. Helium appears to be the most beneficial environment for calcination, although heating in a hydrogen stream produces a catalyst which has a short-lived effectiveness. The hydrogen may increase the number of weakly bound acidic sites which are attached to the catalytic surface at positions not normally occupied by hydrogen. These would be expected to be readily removed but not easily replaced. The calcination in air considerably reduces the activity of the catalyst, possibly due to extraction of acidic sites by oxygen. The calcination in helium may have the effect of removing some of the more highly acidic Brønsted acidic sites, thus producing a beneficial shift in the acid site distribution.

Anderson *et al.* (*31*) have concluded that the C–H bonds in methanol are nonlabile, at least initially. Although the catalyst studied by these workers was the zeolitic ZSM, nevertheless their conclusion may be expected to have some relevance to heteropoly acids, where strong Brønsted acidic sites also appear to be extant. In earlier work on ZSM-5, Chang and Silvestri (*30*) postulated that both acidic and basic sites are active in the production of a carbene-like intermediate. However, Derouane *et al.* (*32*) argue for the initial formation of an ethyl-carbenium ion, which exists on the surface as an ethoxy group. This may desorb as ethylene or react with methanol or dimethyl ether or with ethylene to form a butenyl-carbenium ion. Most recently, Ono and Mori (*33*) conclude that on ZSM-5, surface methoxy groups are formed by the reaction of surface hydroxyl groups and methanol molecules. In contrast to Anderson these authors suggest that methyl carbonium ions then desorb from the methoxy groups and attack the C–H bond of methanol or dimethyl ether molecules.

Heteropoly acids and ZSM-5 catalysts clearly possess strongly acidic sites, although there is evidence (*5*) that the former catalysts may possess a more restricted range of acidic strengths than the latter. However, from the present work it is evident that heteropoly acids do not possess the regular and reproducible distribution of pore sizes found with the Zeolitic ZSM catalysts. Presumably, however, the initiation mechanism with both catalysts can reasonably be expected to be similar, in view of the similarity of the products from each catalyst. Of course, the advantageous restriction of the sizes of molecules permitted to gain entry to the pore structure of ZSM-5 and the additional deterent to the production of molecules which are likely precursors to carbon formation on the surface are not characteristics of the heteropoly acids.

With the heteropoly acids studied here, in particular 12-tungstophosphoric acid, the dimethyl ether molecule appears to act as the precursor to the hydrocarbons with two or more carbon atoms, in a process which presumably involves Brønsted sites

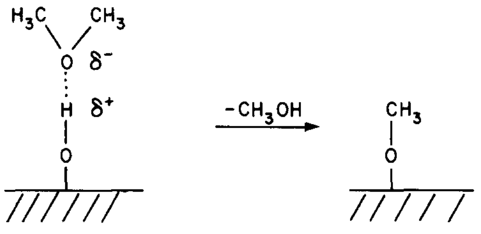

The methoxy group is capable of suffering further reactions in the same manner

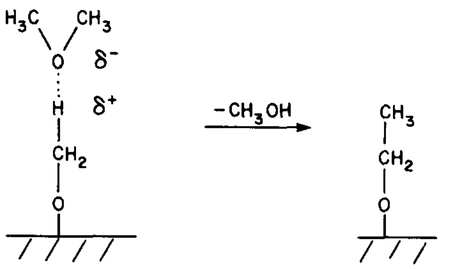

Thus the carbon chain may oligomerize

through the interaction of additional dimethyl ether molecules as well as desorbed species with the surface species. The process of oligomerization is evidently in competition with that of cracking. Shorter residence times remove longer hydrocarbon chains prior to complete degradation while longer residence times provide an opportunity for both extensive cracking and carbonization to occur.

ACKNOWLEDGMENTS

The financial support of the Natural Science and Engineering Research Council of Canada is gratefully acknowledged. The technical assistance of H. Grisebach and J. Young is much appreciated.

REFERENCES

1. See, for example, Miyata, H., and Moffat, J. B., *J. Chem. Soc. Faraday Trans. I.* **77,** 2493 (1981); Moffat, J. B., *in* "Topics in Phosphorus Chemistry" (M. Grayson and E. J. Griffith, Eds.), Vol. 10. Wiley, New York, 1980, and references contained therein.
2. Moffat, J. B., and Gallace, B., *J. Catal.,* **76,** 182 (1982); Moffat, J. B., and Jewur, S. S., *J. Chem. Soc. Faraday Trans. I* **76,** 746 (1980).
3. "Gmelins: Hanbuch der Anorganischem Chemie." System Number 53. Verlag Chemie, Berlin, 1935.
4. Tsigdinos, G. A., *in* "Heteropoly Compounds, Vol. 8, Methodicum Chimicum" (F. Korte, Ed.), Chap. 32. Academic Press, New York, 1976.
5. Tsigdinos, G. A., *Topics Current Chem.* **76,** 1 (1978).
6. Tsigdinos, G. A., "Molybdenum Chemicals Bulletin, cdb-12a (revised)." Climax Molybdenum Co., Ann Arbor, Mich., 1969.
7. "Molybdenum Catalyst Bibliography, Suppl. No. 5." Climax Molybdenum Co., Ann Arbor, Mich., 1978.
8. Eguchi, K., Aso, I., Yamazoe, N., and Seiyama, T., *Chem. Lett.* 1345 (1979).
9. Furuta, M., Sakata, K., Misono, M., and Yoneda, Y., *Chem. Lett.* 31, (1979).
10. Matveev, K. I., Zhizhina, E. G., Shitova, H. B., and Kuznetsova, L. I., *Kinet. Katal.* **18,** 380 (1977).
11. Onoue, Y., Mizutani, Y., Akiyama, S., and Izumi, Y., *Chemtech* July, 432 (1978).
12. Nomiya, K., Ueno, T., and Miwa, M., *Bull. Chem. Soc. Japan* **53,** 927 (1980).
13. Izumi, Y., and Hayashi, K., *Chem. Lett.* 787 (1980).
14. Katamura, K., Nakamura, T., Sakata, K., Misono, M., and Yoneda, Y., *Chem. Lett.* 89 (1981).
15. Ono, Y., Mori, T., and Keii, T., *Intern. Congr. Catal. Tokyo, 1980,* **7.**
16. Baba, T., Sakai, J., Ono, Y., and Keii, T., 47th Meeting of the Catalysis Society of Japan; *Shokubai* **23,** 108 (1981); *J. Chem. Soc. Chem. Commun.* 400 (1981).
17. Wu, H., *J. Biol. Chem.* **43,** 189 (1920).
18. Hayashi, H., and Moffat, J. B., Talanta, in press.
19. Benesi, H. A., and Winquist, B. H. C., *Adv. Catal.* **27,** 97 (1978).
20. Grutter, B., and Jander, G., *in* "Handbook of Preparative Inorganic Chemistry" (G. Brauer, Ed.), 2nd Ed., Vol. 2, p. 1721. Academic Press, New York, 1965.
21. Bradley, A. J., and Illingsworth, J. W., *Proc. R. Soc. (London)* **A157,** 113 (1936).
22. Brown, D. H., *J. Chem. Soc.* 3189 (1962).
23. Otake, M., and Onoda, T., *Shokubai* **18,** 169 (1976).
24. Keggin, J. F., *Proc. R. Soc. (London)* **A144,** 75 (1934).
25. West, S. F., and Audrieth, L. F., *J. Phys. Chem.* **59,** 1069 (1955).
26. Rossini, F. D., Wagman, D. D., Evans, W. H., and Jaffe, I., "Selected Values of Chemical Thermodynamic Propertie." NBS Circular 500 (1961).
27. Dean, J. A. (Ed.). "Lange's Handbook of Chemistry," 12th Ed. McGraw-Hill, New York, 1979.
28. Benson, S. W., Cruickshank, F. R., Golden, D. M., Hangen, G. R., O'Neal, H. E., Rogers, A. S., Shaw, R., and Walsh, R., *Chem. Rev.* **69,** 279 (1969).
29. Ivash, E. V., Li, J. C. M., and Pitzer, K. S., *J. Chem. Phys.* **23,** 1814 (1955).
30. Chang, C. D., and Silvestri, A. J., *J. Catal.* **47,** 249 (1977).
31. Anderson, J. R., Mole, T., and Christon, V., *J. Catal.* **61,** 477 (1980).
32. Dejaifve, P., Vedrine, J. C., Bolis, V., and Derouane, E. G., *J. Catal.* **63,** 331 (1980).
33. Ono, Y., and Mori, T., *J. Chem. Soc. Faraday Trans. 1* **77,** 2209 (1981).